doi:10.1006/jmbi.2000.3998 available online at http://www.idealibrary.com on IDEAL® *J. Mol. Biol.* (2000) **301**, 1029–1039

JMB

Temperature-dependent Equilibrium between the Open and Closed Conformation of the p66 Subunit of HIV-1 Reverse Transcriptase Revealed by Site-directed Spin Labelling

Oliver Kensch, Tobias Restle, Birgitta M. Wöhrl, Roger S. Goody and Heinz-Jürgen Steinhoff*

Max-Planck-Institut für molekulare Physiologie Abteilung Physikalische Biochemie, Otto-Hahn-Straße 11, 44227 Dortmund Germany

**Corresponding author*

X-ray crystallographic studies of human immunodeficiency virus type 1 reverse transcriptase complexed with or without substrates or inhibitors show that the heterodimeric enzyme adopts distinct conformations that differ in the orientation of the so-called thumb subdomain in the large subunit. Site-directed spin labelling of mutated residue positions W24C and K287C is applied here to determine the distances between the fingers and thumb subdomains of liganded and unliganded RT in solution. The inter-spin distances of a DNA/DNA and a pseudoknot RNA complexed reverse transcriptase in solution was found to agree with the respective crystal data of the open and closed conformations. For the unliganded reverse transcriptase a temperature-dependent equilibrium between these two states was observed. The fraction of the closed conformation decreased from 95% at 313 K to 65% at 273 K. The spectral separation between the two structures was facilitated by the use of a perdeuterated [^{15}N]nitroxide methane-thiosulfonate spin label.

Keywords: HIV-1; reverse transcriptase; RNA pseudoknot; EPR spectroscopy; site-directed spin labelling

Introduction

Reverse transcriptase (RT) is a key enzyme in the replication cycle of the human immunodeficiency virus type 1 (HIV-1), catalysing the conversion of virally encoded RNA into proviral DNA (Skalka & Goff, 1993). This essential step in the retroviral life cycle is targeted by a variety of drugs in clinical use to combat AIDS. The RT is a heterodimeric enzyme with subunits of 66 and 51 kDa, respectively. The p66 subunit consists of fingers, palm and thumb subdomains, named according to their resemblance to a right hand, as well as connection and ribonuclease H (RNaseH) subdomains. The smaller subunit, p51, originates from p66 by proteolytic cleavage of the C-terminal RNaseH domain. As a consequence, both subunits have the same amino acid sequence. However, the structural organisation of the subdomains is very much different, resulting in an asymmetric dimer with only one active site per heterodimer localised within the large subunit. During catalysis of the conversion of single-stranded viral RNA into double-stranded DNA, RT has to bind successively the following different primer/templates (p/t): tRNA/RNA, DNA/RNA, RNA/DNA and DNA/DNA. In order to accommodate these substrates, which differ significantly in their structures, the enzyme must have a remarkable intrinsic flexibility. This flexibility is believed to be achieved in part by the above mentioned distinct domain organisation, which is revealed by several crystal structures (Jäger *et al.*, 1994). X-ray structures of unliganded HIV-1 RT, RT bound to a pseudoknot RNA inhibitor, to different non-nucleoside inhibitors (NNRTIs) and to a DNA/DNA p/t have been solved (for a recent review, see Jäger & Pata, 1999). The most striking difference among these structures concerns the position of the p66 thumb subdomain, which undergoes a 30-40° rigid-body

Abbreviations used: EPR, electron paramagnetic resonance; MTSSL, (1-oxyl-2,2,5,5-tetramethylpyrroline-3-methyl) methane thiosulfonate; p/t, primer/template DNA; R1, MTS spin label side-chain; RNase H, ribonuclease H; RT, reverse transcriptase.

E-mail address of the corresponding author: hjs@bph.ruhr-uni-bochum.de

0022-2836/00/041029–11 $35.00/0

movement relative to the p66 palm subdomain on going from the unliganded enzyme to the nucleic acid substrate bound form. This results in an overall opening of the structure, generating a large nucleic acid binding cleft stretching from the N-terminal polymerase core to the C-terminal RNaseH active site. The conformations are designated closed and open, respectively. The positions of the other subdomains remain largely unchanged. In the crystal structures of ligand free RT and RT in complex with a pseudoknot RNA inhibitor, the p66 thumb and fingers subdomains are positioned close together (Rodgers *et al*., 1995; Jäger *et al*., 1998). In this conformation the substrate binding cleft is blocked. On the other hand, in the open state, where the tip of the thumb subdomain moves about 2.5 nm away from the tip of the finger the enzyme is able to accommodate different substrates, as seen in structures of RT in complex with dsDNA (Jacobo-Molina *et al*., 1993; Huang *et al*., 1998) or different NNRTIs (Kohlstaedt *et al*., 1993; Ren *et al*., 1995; Das *et al*., 1996). In one particular instance the open conformation is also found in a crystal structure of unliganded RT (Esnouf *et al*., 1995). Here however, the unliganded structure was a result of soaking out a non-nucleoside inhibitor from a pre-grown crystal.

As yet there is no experimental evidence as to whether unliganded RT adopts the open or the closed conformation in solution. If both conformers, the open and the closed, have similar energies, they may be thermally populated in solution at equilibrium. As outlined above, the X-ray studies would suggest that RT adopts a closed conformation. However, it is possible that the conformation of ligand free RT and NNRTI-bound RT could be influenced by crystal packing, freezing the enzyme in a certain structural state, as indicated by the two different conformations found in the absence of ligands (e.g. closed *versus* open; Rodgers *et al*., 1995; Esnouf *et al*., 1995; Hsiou *et al*., 1996). Madrid *et al*. (1999) performed molecular dynamics simulations recently on the p66 thumb movement starting with the thumb in the upright (open) position. The simulations showed a large subdomain rearrangement where the thumb closes down on the fingers as seen in the crystal structures. It has been proposed that this flexibility may play an essential role in the polymerisation process, enabling the growing nucleic acid chain to translocate along the enzyme after each nucleotide incorporation step.

In this study we used site-directed spin labelling to analyse the conformational states in solution of unliganded RT and RT bound either to a model DNA/DNA p/t or an RNA inhibitor. In particular, we were interested in answering the question of whether or not ligand-free RT adopts the closed conformation in solution. Site-directed spin labelling has emerged as a powerful technique for exploring the structure and dynamics of soluble, as well as membrane, proteins (for reviews, see Hubbell *et al*., 1996, 1998). Here, cysteine residues introduced by site-directed mutagenesis at certain positions are modified with specific nitroxide spin labels. The dynamics of this nitroxide side-chain and its accessibility to paramagnetic quenchers allows determination of the identity and orientation of the secondary structure of protein domains and the topography of polypeptide chains with respect to the membrane water interface. Domain motions have been disclosed by measurements of intra-molecular distances and distance changes determined through the dipole-dipole interaction of two spin labels introduced into the protein (Farrens *et al*., 1996; Steinhoff *et al*., 1997; Thorgeirsson *et al*., 1997; Tiebel *et al*., 1999). Here, a detailed analysis of the spin-spin interaction of two nitroxide molecules bound to the fingers and thumb domains of HIV-1 RT allows determination of the conformation of ligand free RT in solution when combined with data obtained from X-ray studies. Our results show that unliganded HIV-1 RT adopts primarily the closed conformation at physiological temperatures in solution. Also, we observe a temperature-dependent equilibrium between the open and closed conformation of the enzyme, indicating a distinct motion of the thumb subdomain. This may have important implications for the translocation process during polymerisation.

Results

Selection of sites for spin-labelled cysteine residues based on the crystal structures of RT

From several crystal structures of HIV RT it is known that the enzyme can adopt essentially two conformations which differ primarily in their orientations of the p66 thumb domain. A superposition of the structures of free RT and DNA/DNA p/t bound RT is shown in Figure 1. In the apo-enzyme structure the tips of the thumb and the fingers subdomains are in close vicinity. In contrast, the crystal structure of RT in complex with DNA/DNA p/t reveals a 30-40 ° rigid-body movement of the thumb subdomain relative to the palm domain compared to the unliganded enzyme, resulting in an open conformation. Additionally, minor reorientations also occur in the RNaseH domain. It is interesting that RT complexed with nevirapine, a non-nucleoside inhibitor, shows an orientation of the thumb subdomain tilted outward leading to a further opening of the substrate-binding cleft.

In order to characterise the conformations of different RT complexes in solution and to compare these findings with the crystal structures, we were interested in determining the distances between the fingers and thumb domains. Since the quantitative analysis of spin-spin interactions between two spin labels is restricted to inter-spin distances of less than 2.5 nm (Steinhoff *et al*., 1997), we chose amino acid residues Trp24 (fingers) and Lys287 (thumb) of p66, which exhibit C^{β}-C^{β} distances of 1.2 nm in the closed conformation and 2.9 or more

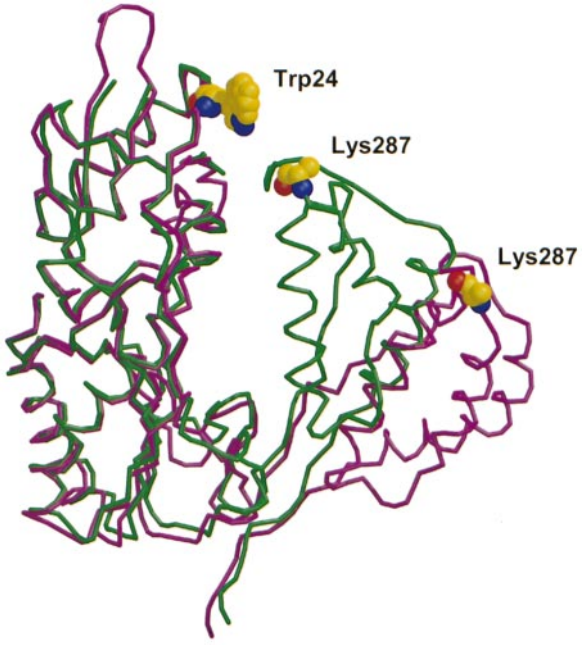

Figure 1. Crystal structures of the fingers and thumb domains of the p66 subunit of HIV-1 RT complexed with dsDNA (purple, Jacobo-Molina *et al*., 1993) and unliganded RT (green, Rodgers *et al*., 1995). The nucleic acid is not shown for clarity. The different orientations of the thumb domain lead to different distances between Trp24 and Lys287 (space filled) which were replaced by spin-labelled cysteine residues in the present work. The C^{β}-C^{β} distance between the native residues at positions 24 in the fingers domain and 287 in the thumb domain determined from the crystal data amounts to 1.2 nm for the unliganded RT and 3.5 nm for the DNA complexed RT.

than 3.0 nm in the open conformations, respectively (Jacobo-Molina *et al*., 1993; Jäger *et al*., 1998; Huang *et al*., 1998). The respective positions of these residues are depicted in the crystal structures shown in Figure 1. These residues were replaced by cysteine residues, while the naturally occurring solvent-accessible cysteine residues at positions 38 (p66) and 280 (p66, p51) were mutated to serine residues. The overall effect of mutagenesis and spin labelling with MTSSL 1-^{15}N-d_{15} on the RNA-dependent DNA polymerase activity was found to be negligible.

Conformation of RT complexes in frozen solution

The spin-spin interaction between two spin labels attached to a protein is composed of static dipolar interaction, modulation of the dipolar interaction by the rotational diffusion of the protein and residual motion of the spin label side-chains as well as exchange interaction. For temperatures below 200 K, the rotational diffusion of the protein and the residual motion of the spin label side-chain is strongly restricted (Steinhoff *et al*., 1989). Static dipolar interaction leads to considerable broadening of the spectrum for inter-spin distances less than 2.5 nm. A detailed line shape analysis allows determination of absolute values of the inter-spin distance (Steinhoff *et al*., 1991, 1997; Rabenstein & Shin, 1995; Thorgeirsson *et al*., 1997). For temperatures above 200 K, the dipolar interaction is modulated by the relative motion of the spin labels. If the reorientation rate of the inter-spin vector can be determined, the inter-residue distances can be estimated even at room temperature (Mchaourab *et al*., 1997). Exchange interaction was found to contribute significantly to the line broadening for distances of less than 1.0 nm, since partial overlap of the nitrogen pi-orbitals of the two interacting nitroxides is required (Closs *et al*., 1992; Fiori & Millhauser, 1995).

EPR spectra of unliganded, DNA/DNA p/t and pseudoknot RNA-complexed RT were measured in frozen solution at a temperature of 170 K to exclude dynamic effects. Powder spectra simulations were performed to determine absolute values of the inter-spin distances according to the method of Steinhoff *et al*. (1997). The frozen protein samples are generally composed of species with different nitroxide orientations and inter-spin distances because of the flexibility of the nitroxide side-chains and the variety of conformations of the spin label binding sites in frozen solution. This is accounted for in the fitting procedure by the assumption of a Gaussian inter-spin distance distribution of average distance, d, and distribution width, σ. The consideration of σ additionally accounts for small amounts of single spin labelled protein molecules. The parameters which describe the EPR spectra in the absence of any spin-spin interaction, i.e. the magnetic tensors, g and A, and the line width parameters were fixed according to the values obtained from fitting of simulated powder spectra to experimental data of single labelled samples.

Figure 2 shows a comparison of the spectra which were normalised to represent an equal number of spins. The spectrum of the single mutant W24R1 can be considered as a reference for an interaction free spectrum. In comparison, the spectral shape of the RT-p/t complex reveals a slightly broader line width and consequently a smaller amplitude due to weak dipolar interaction. The spectrum of unliganded RT exhibits a similar shape indicating a similar distance between the fingers and thumb subdomains at this temperature. The line shape was found to be independent of the speed of freezing, with a maximum cooling rate of about 50 K/second. The average inter-spin distance determined from the fitting of simulated spectra exceeds 1.9 nm for the RT-p/t complex and equals 1.8 nm for the unliganded RT. The distribution width σ was found to vary between 0.5 and 0.7 nm. According to the crystal structure, the bound p/t fixes the thumb subdomain in an open conformation with a distance between the C^{β}

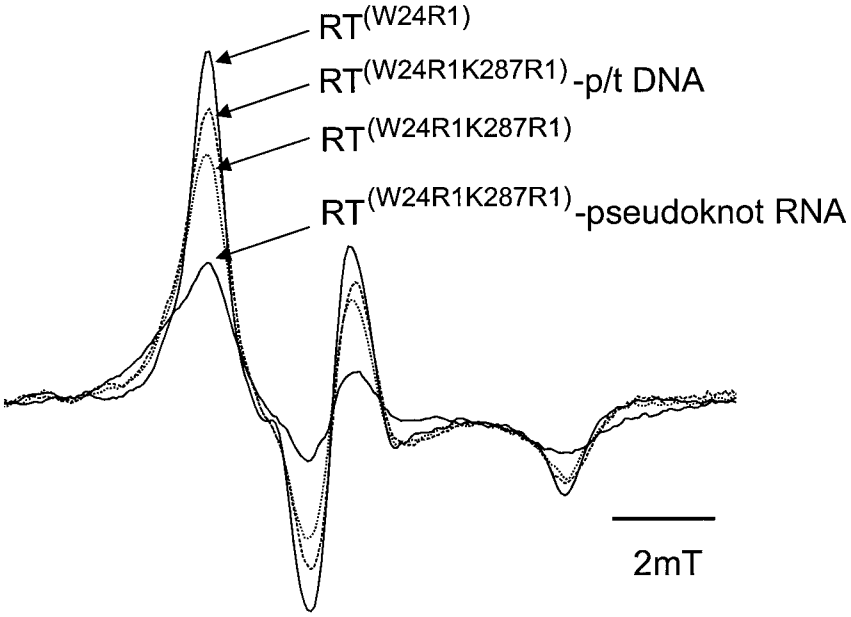

Figure 2. EPR spectra of singly and doubly spin-labelled HIV-1 RT determined at 170 K (first derivative representation). The spectra are normalised to constant spin number. Substantial line broadening due to spin-spin interaction is visible in the spectrum of the W24R1/K287R1 RT complexed with the pseudoknot RNA.

atoms of W24 and K287 of about 2.9 nm in the crystal structure described by Huang *et al*. (1998) and 3.5 nm in the structure solved by Jacobo-Molina *et al*. (1993). An open conformation was also reported for a crystal structure of unliganded RT (Esnouf *et al*., 1995). It should be noted that distances concluded from spin-spin interaction are between the electron spins located in the pi-orbital of the nitroxide nitrogen atoms. Considering a length of the spin label side-chain of approximately 0.7 nm, the experimental data obtained with the RT p/t complex and with the unliganded RT are in agreement with the open conformation found in the crystal structures. In contrast, the RT-pseudoknot RNA complex exhibits considerable line broadening which must be due to strong spin-spin interactions (cf. Figure 2). The average inter-spin distance for this complex in frozen solution was determined from fitting of simulated spectra to be 1.15 nm ($\sigma = 0.5$ nm). This result requires the distance between the fingers and thumb subdomains to be considerably decreased in the RT-pseudoknot RNA complex compared to that in the RT-p/t complex. In order to decide whether the fingers-thumb conformation as seen in the crystal of the RT-pseudoknot RNA complex (Jäger *et al*., 1998) would account for the frozen solution data, molecular dynamics simulations were performed according to the method described by Steinhoff *et al*. (1997, 2000). These simulations allow the estimation of the accessible space for the nitroxide side-chains and the occupancy of different nitroxide orientations. During these calculations, the amino acid residues at positions 20 to 28 and 284 to 290 were free to move, whereas the positions of all other atoms were constrained according to the crystal data (Jäger *et al*., 1998). Evaluation of the nitroxide trajectories of 4 ns length yields an average inter-spin distance of 1.0 nm ($\sigma = 0.3$ nm). Considering an uncertainty of the distance values of ~10 %, the results of the MD simulations agree well with the EPR data. The slightly smaller values of the simulated distance and distribution width compared to the respective values found in frozen solution may indicate a residual flexibility of the fingers and thumb subdomains in the RT-pseudoknot RNA complex in solution which is not accounted for in our simulations.

Conformation of RT complexes in liquid solution

At room temperature ($T = 297$ K) the side-chain motion of the spin label occurs in the ns time range, and the mobility of the nitroxide group as well as the flexibility of its binding site are directly reflected in the EPR absorption line shape. Figure 3 shows the spectra of the singly labelled unliganded and liganded RT mutants W24R1 and K287R1. The spectra of both the W24R1-p/t and -pseudoknot complexes are nearly indistinguishable from the spectrum of the unliganded W24R1. Neither the DNA/DNA p/t nor the pseudoknot RNA interact significantly with the nitroxide bound to position 24. Furthermore, the conformational change from the open (RT-p/t complex) to the closed (RT-pseudoknot complex) conformation (see below) does not alter the interaction of the spin label with the secondary or tertiary structure. A slightly different picture emerges for K287R1. The free RT and the pseudoknot complex show identical spectra, whereas the spin label mobility in the case of the RT-p/t complex is increased. Binding of p/t and the resulting conformational change of RT obviously reduces the interaction of the spin label with neighbouring structures. Although the change of the nitroxide mobility is small, the reorientational correlation time determined from fitting of

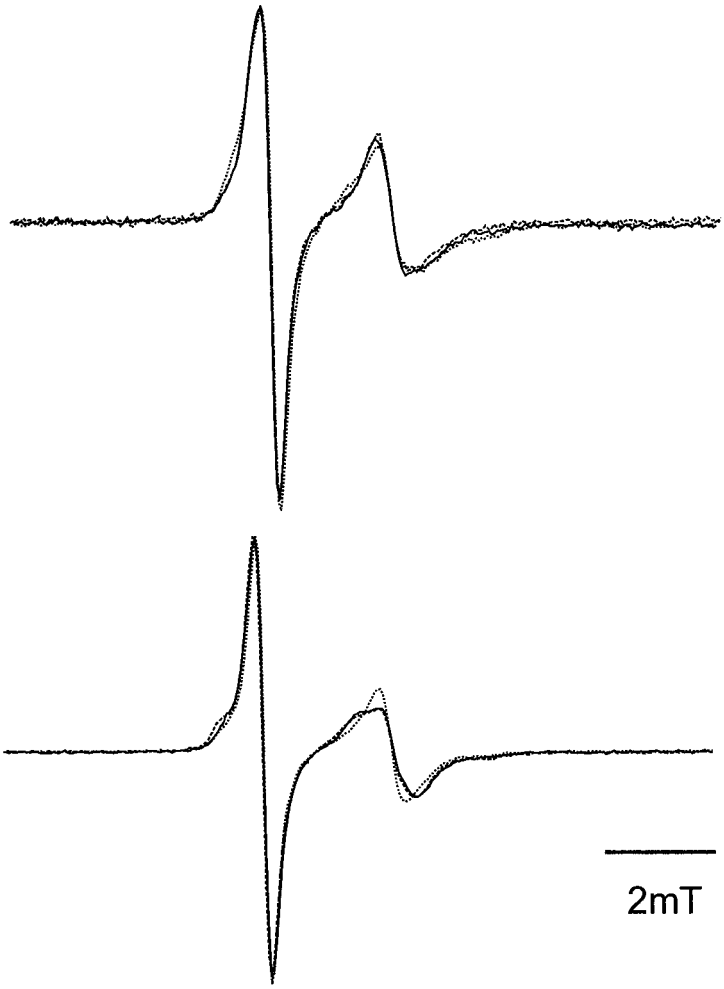

Figure 3. Room temperature EPR spectra (first derivative representation, 294 K) of the singly spin labelled RT W24R1 (top) and K287R1 (bottom). The spectra of the uncomplexed RT (continuous line), DNA complexed RT (dotted line) and pseudoknot RNA liganded RT (broken line) are normalised to constant amplitude.

simulated spectra to the experimental data show a decrease of 25%. For all other samples, fitting of the rotational correlation time with the assumption of isotropic reorientational motion yields values between 1.6 and 1.9 ns. In summary, the mobility of both nitroxide side-chains is found to be in agreement with their location in loop regions (Mchaourab *et al*., 1997; Pfeiffer *et al*., 1999).

Figure 4 shows EPR spectra of the doubly spin-labelled RT complexes. The spectrum of the doubly spin labelled DNA/DNA complexed RT is essentially identical with the spectra of W24R1 and K287R1 (Figure 4(a)). The small deviations in the high field region are due to a small amount of unbound spin label present in the double mutant sample. Hence, spin-spin interaction between the spin-labels is not observable in this complex. The spectra of the doubly labelled unliganded RT (Figure 4(b)) and of the RT-pseudoknot complex (Figure 4(c)) each exhibit a dominating spectral component which is substantially broadened compared to the superposition of the single mutant spectra. Double integration reveals the fraction of this broadened component to exceed 80% for the RT-pseudoknot complex and 70% for the free RT. Spectral simulations confirm that the nature of this line shape cannot be due to further restrictions of the reorientational motion of the spin label side-chains but must originate from spin-spin interaction between the nitroxide groups. Convolution of the spectra of the single mutants with a Lorentian broadening function reveals the additional broadening of the spectrum of the doubly spin labelled RT-pseudoknot complex to approach 6.5 G. A superposition of the spectra of the RT-pseudoknot complex with that of the RT-p/t complex with a fraction ratio of 9 to 1 agrees excellently with the spectrum of the free RT (cf. Figure 4(b)). The strengths of the spin-spin interaction are identical for the interacting fractions in the free and pseudoknot complexed RT. This is strong evidence that the distances between the fingers and the thumb domains in these fractions are very similar. However, the species which lack spin-spin interaction are different in both samples. This will be addressed below.

Initially, we estimated the distance between the nitroxide groups in the RT complexes in liquid solution and compared this value with the data determined for the frozen solution. The spectral shapes

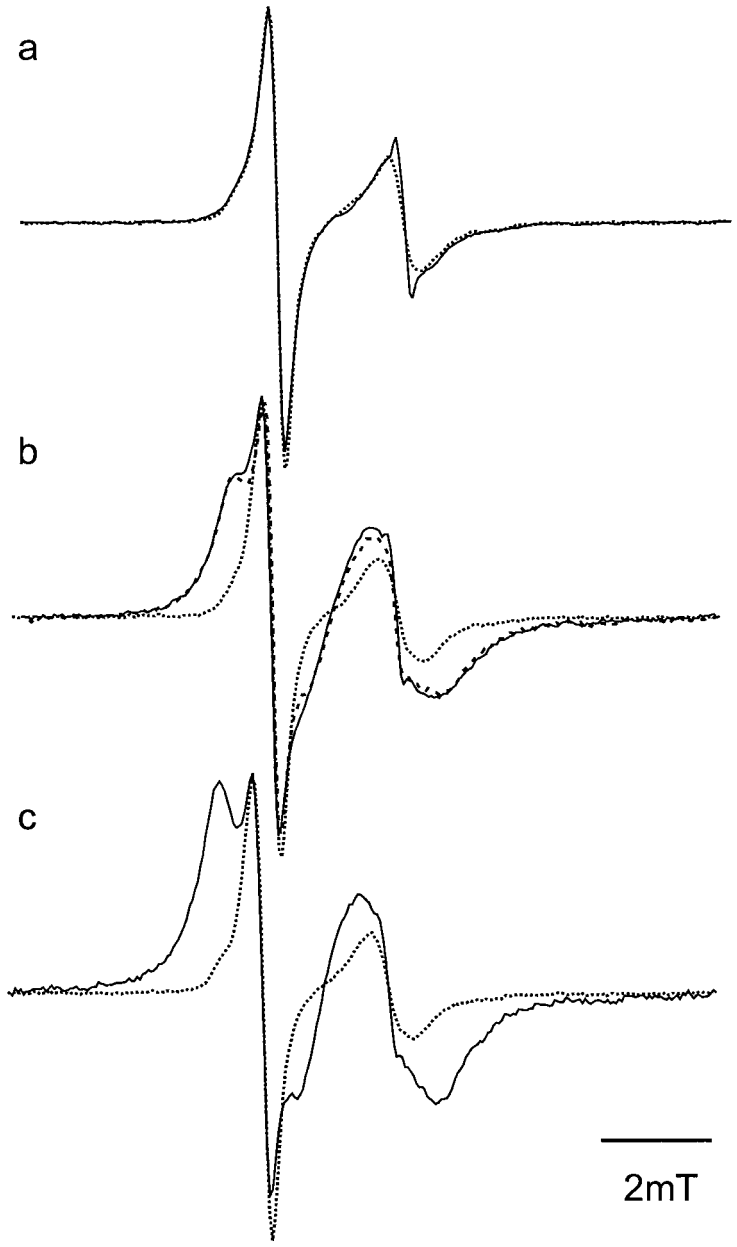

Figure 4. Room temperature spectra of the doubly spin-labelled RT complexes (continuous line) compared to a superposition of spectra of the respective singly labelled RT complexes (dotted line). All spectra are normalised to constant amplitude of the low field line. (a) RT complexed with duplex DNA; (b) uncomplexed RT; and (c) RT complexed with pseudoknot RNA. Compared to the superposition spectra the line shape of the uncomplexed RT and of RT complexed with pseudoknot RNA is dominated by an additional broad component. A superposition of 90 % (spin number) of the spectrum of the pseudoknot complexed RT with 10 % of that of the DNA complexed RT is shown in (b) as a broken line. Its shape is in agreement with the experimental spectrum of the doubly labelled uncomplexed RT.

of the single mutants correspond to nitroxide groups near the fast motional limit. In this regime the spectral anisotropies are averaged and the homogeneous line widths are determined by modulation of the anisotropic hyperfine and Zeeman interactions due to molecular motion. Relaxation due to static and dynamic dipolar interaction and exchange interaction must be considered additionally for the doubly spin-labelled samples. For rotational correlation times less than $2\hbar r^3/3g^2\beta^2$, where $\hbar$ is the Planck constant divided by 2 π, g and β are the g factor and the Bohr magneton, and r is the inter-spin distance, the static dipolar contribution is averaged. If we assume the rotational correlation time of the inter-spin vector in RT to equal that of the protein rotational diffusion, ~50 ns (in water at room temperature), static dipolar effects are averaged only for inter-spin distances exceeding 3 nm. Static dipolar line broadening should dominate the spectra of RT for inter-spin distances less than 2 nm and temperatures below room temperature. Simulations of dipolar broadened spectra are in agreement with the broad component of the experimental line shape of the pseudoknot complexed RT for inter-spin distances ranging from 1.1 nm at 272 K to 1.4 nm at 313 K. The line width decrease with increasing temperature is strong evidence that exchange interaction does not significantly contribute but the inter-spin vector is modulated by the residual motion of the spin labels. This may partially average the dipolar interaction at higher temperatures and hence lead

to an apparent increase of the calculated inter-spin distance (Steinhoff *et al*., 1991). The results of the simulations are therefore in excellent agreement with the value of 1.15 nm determined for the pseudoknot complexed RT in frozen solution. Furthermore, our result shows the RT-pseudoknot-RNA complex to adopt the closed conformation at room temperature. The distance between the fingers and thumb subdomains of the dominating fraction of the unliganded RT must be very similar, since the corresponding spectral shape is indistinguishable from that of the RT-pseudoknot complex. This finding is in contrast to the low temperature data, where the unliganded RT was shown to adopt an open conformation. This contradiction led us to the conclusion, that the conformation of the unliganded RT may be temperature dependent.

Temperature dependence of the EPR spectra

A series of EPR spectra of the singly and doubly spin-labelled RT complexes were recorded at six different temperatures between 272 K and 313 K. The fraction of the interacting species in the pseudoknot-RNA complexed RT was determined from the integrated spectra. This fraction amounted to 70-80 % for different preparations and varied less than 5 % with temperature over the whole range studied. A reasonable explanation for the non-interacting fraction in the RT-pseudoknot complex is the incomplete spin labelling (efficiency 85-90 %; see Materials and Methods). Assuming a similar reaction efficiency for both spin label binding sites, the square value yields the probability of finding interacting pairs of nitroxide groups, i.e. 70-81 % of the molecules should show spin-spin interaction in agreement with the experimental results.

A completely different picture evolves for the unliganded RT. The fraction showing spin-spin interaction varies between 65 % at 272 K and 95 % at 313 K. This is proof of a temperature-dependent equilibrium of two different conformations of free RT. For each temperature studied the EPR line shape of the free RT could be reasonably well simulated by a superposition of the spectra of the DNA/DNA and pseudoknot complexed RT (cf. Figure 4(b)). The fraction of free RT showing spin-spin interaction must adopt a conformation with the distance between the fingers and thumb domains identical to that found in the RT pseudoknot RNA complex and is therefore identified as the closed conformation. The other fraction exhibits an inter-spin distance of more than 1.9 nm and thus the conformation may be similar or identical to that of the RT p/t complex, i.e. the open conformation. The logarithm of the equilibrium constant for the transition between the open and closed conformation exhibits a linear dependence with the inverse temperature (Figure 5). Entropy and enthalpy values determined from the intercept and the slope amount to 134(±10) J/mol K and 34.5(±3) kJ/mol, respectively.

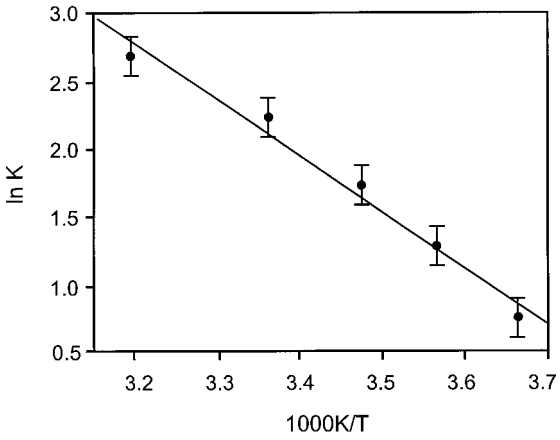

Figure 5. Plot of the ratio of the fractions of the closed and open structures of the uncomplexed HIV-1 RT *versus* inverse temperature. The error is mainly due to uncertainties in spectra integration. The fraction of the closed conformation decreases from 95 % at 313 K to 65 % at 273 K. The reaction enthalpy and entropy determined from the slope and intercept of the regression line amount to 34.5(±3) KJ/mol and 134(±10) J/mol K, respectively.

Conformation of RT-NNRTI complexes in solution

As the developed technique of double spinlabelling RT was found to be a useful tool to examine the conformation of the p66 subunit, we additionally examined the conformation of two RT NNRTI complexes in solution. Figure 6 shows the EPR spectra of nevirapine and S-TIBO (a TIBO derivative) bound to RT (Merluzzi *et al*., 1990; Pauwels *et al*., 1990). Comparing these spectra with a superposition of spectra of the singly labelled RT yields no indication for spin-spin interaction. Therefore, nevirapine-complexed as well as S-TIBO-complexed RT adopt an open conformation in solution, which must be stabilised *via* the bound inhibitor. This finding is in agreement with the crystal structure of a RT nevirapine complex (Kohlstaedt *et al*., 1993) and the X-ray data of 8-Cl and 9-Cl-TIBO (Das *et al*., 1996).

Discussion

The available crystal structures of unliganded RT and RT complexes with substrate show one most striking difference. Comparing the structure of RT complexed with dsDNA and the unliganded RT reveals a rotation of the thumb domain of about 30-40° closing off the DNA-binding cleft and representing a transition from an open to a closed state (Jacobo-Molina *et al*., 1993; Rodgers *et al*., 1995). In addition, minor structural changes occur in the RNaseH domain. For the unliganded RT two crystal structures have been solved, showing two different conformations. The closed

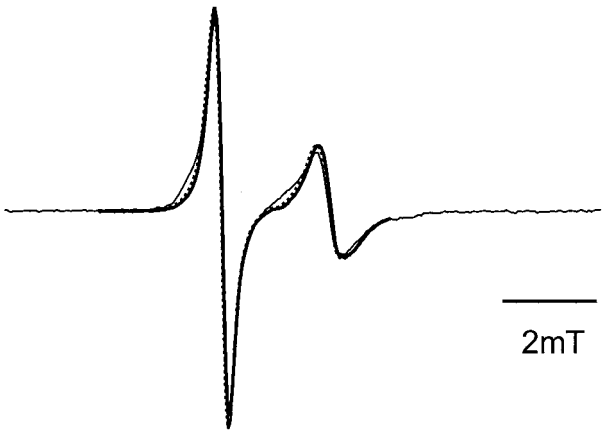

Figure 6. EPR spectra of doubly spin-labelled RT complexed with nevirapine (continuous line) and S-TIBO (a TIBO derivative, broken line). The thin line shows the superposition of the two singly spin-labelled RT mutants.

conformation is seen in the structures solved by Rodgers *et al*. (1995) and Hsiou *et al*. (1996), whereas Esnouf *et al*. (1995) determined a structure showing an open conformation. Here however, the unliganded structure was produced by soaking out a weak binding non-nucleoside inhibitor, HEPT, from a pregrown crystal. It cannot be excluded that the open conformation is stabilised by crystal packing. The objective of the present work was to answer the question as to which of these conformations (open and/or closed) exists in solution.

Initially, we analysed the inter-spin distances of two nitroxide spin labels attached to the fingers and thumb domains of p66 of the heterodimeric enzyme complexed with an RNA pseudoknot inhibitor. This RNA aptamer was originally identified *via* SELEX by Tuerk *et al*. (1992). More recently the structure of this enzyme/aptamer complex was solved (Jäger *et al*., 1998). The RNA ligand-binding surface lies within the nucleic acid cleft of the enzyme, between the polymerase and RNaseH active sites, and partially overlaps the binding surface of duplex DNA substrates. The protein/RNA interaction was shown to stabilise the closed conformation of the enzyme through electrostatic interactions between the p66 thumb and the RNA and therefore chosen as a reference for this structural state. Binding studies revealed an extraordinarily low K_d of about 25 pM for the enzyme/aptamer interaction coupled with high specificity (Kensch *et al*., 2000). Using EPR spectroscopy in combination with site-directed spin labelling, we could show that the distance between nitroxide side-chains attached to positions 24 and 287 in the fingers and thumb domains of a pseudoknot complexed RT in solution are in good agreement with distance values determined from the crystal structure. The observed inter-spin distances in the presence of the RNA aptamer were constant within the analysed temperature range (170 K-313 K) in contrast to the situation with unliganded enzyme (see below). This clearly demonstrates that the pseudoknot RNA shifts the open/closed equilibrium by fixing the thumb in the closed conformation. As a consequence, this potent inhibitor not only partly occupies the nucleic acid binding cleft but also stabilises a conformation of the enzyme, which makes it impossible for the natural substrate to bind.

In a subsequent experiment we compared these findings to the situation were the nucleic acid substrate is bound to RT. At present, two different crystal structures are available for HIV-1 RT in complex with dsDNA. The first, RT in complex with an 18/19mer DNA/DNA p/t (Jacobo-Molina *et al*., 1993), is partly shown in Figure 1 (purple). The second is composed of RT covalently linked to a 21/25mer DNA/DNA p/t and a dNTP bound in the polymerase active site (Huang *et al*., 1998). Here, compared to the complex without dNTP, the fingers domain is bent towards the thumb domain which leads to a decrease of 0.6 nm in the distance between the C^{β} of W24 (fingers) and K287 (thumb) from 3.5 nm to 2.9 nm. Fits of the EPR spectrum of the doubly labelled RT W24R1/K287R1 in complex with an 18/36mer p/t provide an average distance of 1.9 nm between the spins in frozen solution. Considering the spin label tether length of 0.7 nm and the spin label side-chains to be oriented head-to-head, the maximum possible C^{β}–C^{β} distance of W24C and K287C is 3.3 nm. Therefore, in frozen solution the distance between the fingers and the thumb domains is probably similar to that observed in the RT-p/t DNA complex with a dNTP bound in the polymerase active site. The room temperature EPR spectrum of the doubly spin-labelled sample is nearly indistinguishable from that of the superposition of the singly spin-labelled samples. Line broadening due to spin-spin interaction must be less than 0.2 Gauss, leading to an inter-spin distance of more than 2 nm. This is in agreement with the low temperature data of an open conformation of the DNA complexed RT.

Finally, we analysed the conformation of RT in the ligand-free state. The EPR spectra of the unliganded RT exhibit two components which are identical to the spectral shapes of the DNA and pseudoknot complexed RT, respectively. The small intrinsic line width of the perdeuterated ^{15}N-MTS spin label and the considerable dipolar broadening facilitated unique separation of the two components. At low temperatures (273 K) 35% of the molecules were found to adopt an open conformation. On increasing the temperature, the fraction of RT molecules showing an open conformation decreases. At physiological temperatures (313 K), 95% of the enzyme molecules show a closed conformation. The distance between the thumb and fingers domains in the closed conformation found in solution agrees with that of the crystal data. The temperature dependence of the equilibrium constant yields a reaction enthalpy of 34.5 kJ/mol for

the switch from an open to the closed state, and an entropy difference of 134 J/mol K.

The EPR spectra of the unliganded RT are superimposable on combination-spectra of the open and the closed conformation for all temperatures measured. We therefore conclude that sub states with inter-spin distances other than those of the open or closed conformation are not populated or have short lifetimes. Shock freezing from 273 K to 170 K yields the open conformation as the predominant fraction. Therefore, the inter-conversion rate between the open and closed states must be fast compared to the rate of cooling. Kinetic experiments to determine the rates are in progress.

In summary, the presented results clearly demonstrate for the first time that the p66 thumb domain of HIV-1 RT is highly flexible in solution adopting two defined conformations, namely an open and a closed conformation, respectively. This is in perfect agreement with the available X-ray structures of the enzyme and confirms that the observed structures are not a result of crystal packing artefacts. At physiological temperatures the open/closed equilibrium is shifted towards the closed conformation whereas at low temperatures the open conformation is energetically favoured. However, the exact biological function of this large domain movement within the catalytic pathway of the enzyme remains to be elucidated. A conceivable scenario would be for this movement to be involved in the translocation of the nucleic acid substrate along the enzyme during polymerisation.

Materials and Methods

Mutagenesis of reverse transcriptase

Initially, all naturally occurring, solvent accessible cysteine residues were replaced by serine residues and the mutant RT $p66^{C38S,C280S}/p51^{C280S}$ was generated. The cysteine residue at position 38 in the small subunit, p51, is not solvent accessible and consequently does not interfere with site-directed labelling. Subsequently, cysteine residues were introduced at the desired positions 24 and 287 in p66 and tagged with a nitroxide spin label.

The mutations were introduced into the plasmids $pRT1_{66}$ (Müller *et al.*, 1989) and p6HRT51 (Le Grice *et al.*, 1991) by site-directed mutagenesis using PCR (Ho *et al.*, 1989). For each mutation, two complementary primers carrying the desired mutated codon (sense and anti primer, respectively) were synthesised. In a first step two separate PCR reactions were carried out, one with the sense, the other with the anti primer, using a second flanking primer in each reaction to generate a fragment which contains a specific restriction site. The products of the two PCR reactions were isolated and hybridised. This hybrid was amplified in a third PCR using the flanking primers from the initial PCR reactions. Subsequently, the resulting DNA fragment containing the desired mutation was digested by two specific restriction enzymes, purified and ligated with the corresponding RT plasmid. Transformation of *Escherichia coli* M15/pDMI.1 (Certa *et al.*, 1986) with the ligated plasmids resulted in expression systems for mutated p66 and mutated his-tagged p51.

Protein purification

Purification of mutant RT was carried out according to a protocol described previously (Wöhrl *et al.*, 1997). Reconstruction of heterodimeric p66/p51 RT was achieved by co-homogenisation of *Escherichia coli* cells expressing p66 and p51, respectively. The purified proteins were dialysed against buffer A, containing 100 mM Tris-HCl (pH 7.0), 25 mM NaCl and 10 % (w/v) glycerol, shock frozen in liquid nitrogen and stored at −80 °C. Mass-spectrometry confirmed the presence of the introduced mutations. Protein concentrations were determined using an extinction coefficient of 260450 M^{-1} at 280 nm. The purified RT was free of nuclease contamination.

Spin labelling of RT mutants

In order to reduce any disulfide bonds, 2 µl of 1 M DTT was added to 200 µl of a 44 µM solution of mutant RT ($p66^{W24C,C38S,C280S,K287C}/p51^{C280S}$) in buffer A containing 300 mM Tris-HCl (pH 7.0). After 30 minutes at 4 °C a twofold excess of 18/36mer DNA/DNA p/t was added to the solution. Excess DTT was separated from the resulting RT-p/t complex using a Sephadex G25 gel filtration column (Pharmacia). The eluted complex was collected in a tube containing 2 µl of 100 mM ^{15}N-d_{15}-(1-oxyl-2,2,5,*S*-tetramethylpyrroline-3-methyl) methanethiosulfonate (MTSSL-^{15}N-d_{15}; Toronto Research Chemicals, Inc.) in DMSO. After 16 hours at 4 °C, the reaction mixture was loaded onto a Ni^{2+}-nitrilotriacetic acid-Sepharose column (Qiagen). Excess spin label and bound p/t were removed from the protein by washing the column extensively with a buffer containing 1 M NaCl and the enzyme was eluted with 0.3 M imidazole. Subsequently, the protein solution was concentrated and buffer was changed (50 mM Tris-HCl (pH 8.0), 25 mM NaCl, 6 mM $MgCl_2$, 10 % glycerol) using centrifugal filters (Millipore). Finally, samples were shock frozen in liquid nitrogen and stored at −80 °C. The labelling efficiency was estimated from double integration of the EPR spectra and absorption measurements of protein (280 nm) and found to be ∼90 %. RNA-dependent DNA polymerase activity of the spin-labelled-mutant protein was determined by a standard RT assay described (Restle *et al.*, 1990; Jacques *et al.*, 1994). The activity of mutant RT on poly(rA)oligo$(dT)_{12\text{-}18}$ substrates was found to be essentially indistinguishable from that of wild-type enzyme. Furthermore, equilibrium binding measurements with a 18/36mer DNA/DNA p/t substrate reveal a K_d of 3 nM for wild-type and 6 nM for the mutant enzyme. Transient kinetic analyses show comparable rates of binding for the mutant and wild-type enzyme (data not shown). Binding assays and transient kinetic analyses were performed as described before (Wöhrl *et al.*, 1999).

EPR measurements

Continuous wave EPR experiments were performed using X-band EPR spectrometers of our own construction equipped with a dielectric resonator (Bruker) or with a H_{103} cavity (AEG). The magnetic field was measured with a B-NM 12 B-field meter (Bruker). Spin-labelled RT samples were loaded into EPR quartz capillaries (50 µl for low temperature measurements, otherwise 5 µl) at a final RT concentration of 100-200 µM. All measurements were performed in a buffer containing 50 mM Tris-HCl (pH 7.0), 12 mM NaCl and 5 % glycerol.

Spectra were recorded with a modulation amplitude of 1.5 G and the microwave power adjusted to be between 0.2 mW and 0.6 mW. A modified Oxford ESR 9 variable temperature accessory allowed stabilisation of the sample temperature between 80 K and 330 K. The EPR spectrometers were controlled by a personal computer, which also performed 12 bit analog-to-digital data acquisition. EPR powder spectra simulations were performed according to the method described by Steinhoff *et al*. (1997).

Acknowledgements

We gratefully acknowledge the support of the Deutsche Forschungsgemeinschaft (SFB 394, C8) and thank C. Beier for MD simulations.

References

Certa, U., Bannwarth, W., Stuber, D., Gentz, R., Lanzer, M., Le Grice, S., Guillot, F., Wendler, I., Hunsmann, G., Bujard, H. & Mous, J. (1986). Subregions of a conserved part of the HIV gp41 transmembrane protein are differentially recognized by antibodies of infected individuals. *EMBO J.* **5**, 3051-3056.

Closs, G. L., Forbes, M. D. E. & Piotrowiak, P. (1992). Spin and reaction dynamics in flexible polymethylene biradicals as studied by EPR, NMR, and optical spectroscopy and magnetic field effect. Measurements and mechanisms of scalar electron spin-spin coupling. *J. Am. Chem. Soc.* **114**, 3285-3294.

Das, K., Ding, J., Hsiou, Y., Clark, A. J., Moereels, H., Koymans, L., Andries, K., Pauwels, R., Janssen, P., Boyer, P., Clark, P., Smith, R. J., Kroeger, S. M., Michejda, C., Hughes, S., *et al.* (1996). Crystal structure of 8-Cl and 9-Cl TIBO complexed with wild-type HIV-1 RT and 8-Cl TIBO complexed with the Tyr181Cys HIV-1 drug-resistant mutant. *J. Mol. Biol.* **264**, 1085-1100.

Esnouf, R., Ren, J., Ross, R., Jones, Y., Stammers, D. & Stuart, D. (1995). Mechanism of inhibition of HIV-1 reverse transcriptase by non nucleoside inhibitors. *Nature Struct. Biol.* **2**, 303-308.

Farrens, D. L., Altenbach, C., Yang, K., Hubbell, W. L. & Khorana, H. G. (1996). Requirement of rigid-body motion of transmembrane helices for light activation of rhodopsin. *Science,* **74**, 768-770.

Fiori, W. R. & Millhauser, G. L. (1995). Exploring the peptide 3(10)-helix reversible alpha-helix equilibrium with double label electron spin resonance. *Biopolymers,* **37**, 243-250.

Ho, S. N., Hunt, H. D., Horton, R. M., Pullen, J. K. & Pease, L. R. (1989). Site-directed mutagenesis by overlap extension using polymerase chain reaction. *Gene,* **77**, 51-59.

Hsiou, Y., Ding, J., Das, K., Clark, A. J., Hughes, S. & Arnold, E. (1996). Structure of unliganded HIV-1 reverse transcriptase at 2.7 Å resolution: implications of conformational changes for polymerization and inhibition mechanisms. *Structure,* **4**, 853-860.

Huang, H., Chopra, R., Verdine, G. & Harrison, S. (1998). Structure of a covalently trapped catalytic complex of HIV-1 reverse transcriptase: implications for drug resistance. *Science,* **282**, 1669-1675.

Hubbell, W. L., McHaourab, H. S., Altenbach, C. & Lietzow, M. A. (1996). Watching proteins move using site-directed spin labeling. *Structure,* **4**, 779-783.

Hubbell, W. L., Gross, A., Langen, R. & Lietzow, M. A. (1998). Recent advances in site-directed spin labeling of proteins. *Curr. Opin. Struct. Biol.* **8**, 649-656.

Jacobo-Molina, A., Ding, J., Nanni, R. G., Clark, A. D. J., Lu, X., Tantillo, C., Williams, R. L., Kramer, G., Ferris, A. L., Clark, P., Hizi, A., Hughes, S. H. & Arnold, E. (1993). Crystal structure of human immunodeficiency virus type 1 reverse transcriptase complexed with double-stranded DNA at 3.0 Å resolution shows bent DNA. *Proc. Natl Acad. Sci. USA,* **90**, 6320-6324.

Jacques, P. S., Wöhrl, B. M., Ottman, M., Darlix, J. L. & Le Grice, S. F. (1994). Subunit-selective mutagenesis indicates minimal polymerase activity in heterodimer-associated p51 HIV-1 reverse transcriptase. *J. Biol. Chem.* **269**, 26472-26478.

Jäger, J. & Pata, J. (1999). Getting a grip: polymerases and their substrate complexes. *Curr. Opin. Struct. Biol.* **9**, 21-28.

Jäger, J., Smerdon, S., Wang, J., Boisvert, D. & Steitz, T. (1994). Comparison of three different crystal forms shows HIV-1 reverse transcriptase displays an internal swivel motion. *Structure,* **2**, 869-876.

Jäger, J., Restle, T. & Steitz, T. A. (1998). The structure of HIV-1 reverse transcriptase complexed with an RNA pseudoknot inhibitor. *EMBO J.* **17**, 4535-4542.

Kensch, O., Connolly, B. A., Steinhoff, H. J., McGregor, A., Goody, R. S. & Restle, T. (2000). HIV-1 reverse transcriptase/pseudoknot RNA aptamer interaction has a binding affinity in the low picomolar range coupled with high specificity. *J. Biol. Chem.* **275**, 18271-18278.

Kohlstaedt, L. A., Wang, J., Friedman, J. M., Rice, P. A. & Steitz, T. A. (1993). Crystal structure at 3.5 Å resolution of HIV-1 reverse transcriptase complexed with an inhibitor. *Science,* **256**, 1783-1790.

Le Grice, S. F., Naas, T., Wohlgensinger, B. & Schatz, O. (1991). Subunit-selective mutagenesis indicates minimal polymerase activity in heterodimer-associated p51 HIV-1 reverse transcriptase. *EMBO J.* **10**, 5-3911.

Madrid, M., Jacobo-Molina, A., Ding, J. & Arnold, E. (1999). Major subdomain rearrangement in HIV-1 reverse transcriptase simulated by molecular dynamics. *Proteins: Struct. Funct. Genet.* **35**, 332-337.

Mchaourab, H. S., Oh, K. J., Fang, C. J. & Hubbell, W. L. (1997). Conformation of T4 lysozyme in solution: hinge-bending motion and the substrate-induced conformational transition studied by site-directed spin labeling. *Biochemistry,* **36**, 307-316.

Merluzzi, V. J., Hargrave, K. D., Labadia, M., Grozinger, K., Skoog, M., Wu, J. C., Shih, C. K., Eckner, K., Hattox, S. & Adams, J. (1990). Inhibition of HIV-1 replication by a non-nucleoside reverse transcriptase inhibitor. *Science,* **50**, 1411-1413.

Müller, B., Restle, T., Weiss, S., Gautel, M., Sczakiel, G. & Goody, R. S. (1989). Co-expression of the subunits of the heterodimer of HIV-1 reverse transcriptase in *Escherichia coli*. *J. Biol. Chem.* **264**, 13975-13978.

Pauwels, R., Andries, K., Desmyter, J., Schols, D., Kukla, M. J., Breslin, H. J., Racymaeckers, A., Van Gelder, J., Woestenborghs, R. & Heykants, J. (1990). Potent and selective inhibition of HIV-1 replication *in vitro*

by a novel series of TIBO derivatives. *Nature,* **343**, 470-474.

Pfeiffer, M., Rink, T., Gerwert, K., Oesterhelt, D. & Steinhoff, H. J. (1999). Site-directed spin-labeling reveals the orientation of the amino acid side-chains in the E-F loop of bacteriorhodopsin. *J. Mol. Biol.* **287**, 163-171.

Rabenstein, M. D. & Shin, Y. K. (1995). Determination of the distance between two spin labels attached to a macromolecule. *Proc. Natl Acad. Sci. USA,* **92**, 8239-8243.

Ren, J., Esnouf, R., Hopkins, A., Ross, C., Jones, Y., Stammers, D. & Stuart, D. (1995). The structure of HIV-1 reverse transcriptase complexed with 9-chloro-TIBO: lessons for inhibitor design. *Structure,* **3**, 915-926.

Restle, T., Müller, B. & Goody, R. S. (1990). Dimerization of human immunodeficiency virus type 1 reverse transcriptase. A target for chemotherapeutic intervention. *J. Biol. Chem.* **265**, 8986-8988.

Rodgers, D. W., Gamblin, S. J., Harris, B. A., Ray, S., Culp, J. S., Helimig, B., Woolf, D. J., Debouck, C. & Harrison, S. C. (1995). The structure of unliganded reverse transcriptase from the human immuno deficiency virus type 1. *Proc. Natl Acad. Sci. USA,* **2**, 1222-1226.

Skalka, A. & Goff, S. (1993). *Reverse Transcriptase*, Cold Spring Harbor Laboratory Press, Cold Spring Harbor, NY.

Steinhoff, H. J., Lieutenant, K. & Schlitter, J. (1989). Residual motion of hemoglobin-bound spin labels as a probe for protein dynamics. *Z. Naturforsch.* **44**, 38-46.

Steinhoff, H.-J., Dombrowsky, O., Karim, C. & Schneiderhahn, C. (1991). Two dimensional diffusion of small molecules on protein surfaces: an EPR study of the restricted translational diffusion of protein-bound spin labels. *EUR. Biophys. J.* **20**, 293-303.

Steinhoff, H. J., Radzwill, N., Thevis, W., Lenz, V., Brandenburg, D., Antson, A., Dodson, G. & Wollmer, A. (1997). Determination of interspin distances between spin labels attached to insulin: comparison of electron paramagnetic resonance data with the X-ray structure. *Biophys. J.* **73**, 3287-3298.

Steinhoff, H. J., Müller, M., Beier, C. & Pfeiffer, M. (2000). Molecular dynamics simulation and EPR spectroscopy of nitroxide side-chains in bacteriorhodopsin. *J. Mol. Liquids,* **84**, 17-27.

Thorgeirsson, T. E., Xiao, W. Z., Brown, L. S., Needleman, R., Lanyi, J. K. & Shin, Y. K. (1997). Transient channel-opening in Bacteriorhodopsin - an Epr study. *J. Mol. Biol.* **273**, 951-957.

Tiebel, B., Radzwill, N., Aung-Hilbrich, L. M., Helbl, V., Steinhoff, H. J. & Hillen, W. (1999). Domain motions accompanying Tet repressor induction defined by changes of interspin distances at selectively labelled sites. *J. Mol. Biol.* **290**, 229-240.

Tuerk, C., MacDougal, S. & Gold, L. (1992). RNA pseudoknots that inhibit human immunodeficiency virus type 1 reverse transcriptase. *Proc. Natl Acad. Sci. USA,* **89**, 6988-6992.

Wöhrl, B. M., Krebs, R., Thrall, S. H., Le Grice , S. F. J., Scheidig, A. J. & Goody, R. S. (1997). Kinetic analysis of four HIV-1 reverse transcriptase enzymes mutated in the primer grip region of p66. Implications for DNA synthesis and dimerization. *J. Biol. Chem.* **272**, 17581-17587.

Wöhrl, B. M., Krebs, R., Goody, R. S. & Restle, T. (1999). Refined model for primer/template binding by HIV-1 reverse transcriptase: pre-steady-state kinetic analysis of primer/template binding and nucleotide incorporation events distinguish between different binding modes depending on the nature of the nucleic acid substrate. *J. Mol. Biol.* **292**, 333-344.

Edited by W. Baumeister

(Received 14 April 2000; received in revised form 29 June 2000; accepted 29 June 2000)